Jon Børre Ørbæk
Roland Kallenborn
Ingunn Tombre
Else Nøst Hegseth
Stig Falk-Petersen
Alf Håkon Hoel
Editors

Arctic Alpine Ecosystems and People in a Changing Environment

with 86 Figures and 10 Tables

Springer

Dr. Jon Børre Ørbæk
Norwegian Polar Institute
Svalbard
P.O.Box 505
9171 Longyearbyen
Norway

Dr. Else N. Hegseth
Norwegian College of Fishery Science
University of Tromsø
Breivika
9037 Tromsø
Norway

Dr. Roland Kallenborn
Norwegian Institute
for Air Research
Polar Environmental Centre
9296 Tromsø
Norway

Dr. Stig Falk-Petersen
Norwegian Polar Institute
Polar Environmental Centre
9296 Tromsø
Norway

Dr. Ingunn Tombre
Norwegian Institute
for Nature Research
Polar Environmental Centre
9296 Tromsø
Norway

Dr. Alf H. Hoel
University of Tromsø
Department of Political Science
Breivika
9037 Tromsø
Norway

Cover photograph: Bjørn Fossli Johansen, Norwegian Polar Institute, 2005

Library of Congress Control Number: 2006935137

ISBN-10 3-540-48512-4 Springer Berlin Heidelberg New York
ISBN-13 978-3-540-48512-4 Springer Berlin Heidelberg New York

Springer is a part of Springer Science+Business Media
springer.com

Cover design: E. Kirchner, Heidelberg
Production: Almas Schimmel
Typesetting: camera-ready by authors
Printing: Krips bv, Meppel
Binding: Stürtz AG, Würzburg

Printed on acid-free paper 30/3141/as 5 4 3 2 1 0

18 Modeling of long-range transport of contaminants from potential sources in the Arctic Ocean by water and sea ice

Vladimir Pavlov

Norwegian Polar Institute, Polar Environmental Centre, N-9296, Tromsø, Norway, e-mail: pavlov@npolar.no

18.1 Introduction

The geographical position and climatic features of the Arctic seas mean that their ecological balance is sensitive to disturbance by inputs of man-made pollutants. The Arctic seas represent zones where pollutants naturally accumulate and pollutants are transported between regions where there is active exploitation of natural resources and pollution, and the ecologically clean regions of the central Polar Basin. The processes involved in the transport, transformation and accumulation of contaminants from different possible sources are important in assessing whether we are to forecast the fate of potential pollutant releases. These sources and potential sources are described by several reports and papers (Yablokov Commission Report 1993; Aarkrog 1993; Pavlov and Pfirman 1995; Duursma and Carroll 1996; ANWAP 1997; AMAP 1997; AMAP 1998; Champ et al. 1998; Yablokov 2001). In some Arctic seas, such as the Barents and Kara seas, there were earlier local sources of anthropogenic origin, connected with the nuclear trials at the test site of Novaya Zemlya and dumping of radioactive waste over their areas. Extensive dumping of nuclear materials in the Kara and Barents seaы marine environment is listed in the Yablokov Commission Report (1993) and in Yablokov (2001). Low level liquid radioactive wastes are stored in the following regions of Russia in large volumes: by the northern fleet in the Kola Peninsula in the Murmansk and Severodvinsk regions, and by the Pacific fleet in the Russian Far East in the naval ship yards at Vladivostok. The combined capacity of all Northern Fleet containers amounts to 10,000 m^3 and annual production is estimated to be about 20,000 m^3. Approximately 30 to 40,000 m^3+ of solid radioactive waste is stored at different sites in the Russian Far East and Northwest

(ANWAP 1997; AMAP 1998; Champ et al. 1998). The discharges of fresh water from the large Arctic rivers that have huge catchment areas draining water from land areas and industrial zones also contribute to the input of pollutants into the Arctic Ocean.

Ocean currents and drifting ice are among the most important mechanisms of pollutant transport (Nürnberg et al. 1994; Emery et al. (1997); Pfirman et al. 1997; Nilsson 1997; Rigor and Colony 1997; Smith et al. 1998; Smith and Ellis 1999; Zhang et al. 2000; Rigor et al. 2002; Zhang et al. 2003; Pfirman et al. 2004a; Pfirman et al. 2004b). Severe natural conditions and the year-round presence of drifting ice make direct full-scale observations of currents difficult and expensive. Numerical modelling, supported and validated by in situ field observations, is therefore the only practical possibility for gaining an understanding of water circulation in the Arctic Ocean on different spatial and temporal scales. Many models describing transport and transformation of various pollutants in the water environment of the Arctic have appeared in recent years inspired by increasing anthropogenic effects, especially in coastal zones (Preller and Cheng 1995; Pavlov et al. 1995; Harms 1997; Scott et al. 1997; AMAP 1998; Nies et al. 1999; Harms and Karcher 1999; Harms et al. 2000; Karcher et al. 2004 and others). In these papers, modelling results for the spreading of contaminants from individual sources, mostly located in the Nordic seas and Kara Sea, were discussed. For example, Harms (1997) has described the application of 3-D, baroclinic circulation models to study the dispersal of radioactivity in the Barents and Kara seas. Release is expected to occur at underwater dump sites for radioactive waste in the Kara Sea, used by the former Soviet Union. To cover the wide range of a possible radionuclide dispersion, two different spatial scales were considered: i) the regional scale, which covered the shelves of the Barents and Kara seas and ii) the local scale, which is focused on the bay where some of the dumping took place. The regional-scale model results have suggested that, even for a worst case scenario, the radioactive contamination of Siberian coastal waters would be relatively small compared to observations in other marine systems (e.g. the Baltic Sea and the Irish Sea). Realistic gradual release scenarios show very low concentrations in the central and eastern Kara Sea. Significant contamination of shelf seas such as the Laptev Sea, the Arctic Ocean or the Barents Sea by radioactive waste dispersion from the Kara Sea seems unlikely.

Nies et al. (1999) presented a review of results from a joint project carried out in Germany in order to assess the consequences to the marine environment from the dumping of nuclear waste in the Kara and Barents seas. The project consisted of experimental work on measurements of radionuclides (^{137}Cs, ^{90}Sr, $^{239+240}$Pu, ^{238}Pu, ^{241}Am) in samples from the Arctic marine environment, and numerical modelling of the potential pathways and dispersion of contaminants in the Arctic Ocean. The role of transport by sea ice from the Kara Sea into the Arctic Ocean was assessed. This transport process might be considered as a rapid contribution of pollutants due to entrainment of contaminated sediments into sea ice, followed by export from the Kara Sea by the Transpolar Ice Drift, and subsequent release in the Arctic Ocean in the region of the East Greenland Current. Numerical modelling of pollutant dispersion from the Kara and Barents seas was carried out both on a local scale, for the Barents and Kara seas, and for long range dispersion into the Arctic and Atlantic oceans. 3-D baroclinic circulation models were applied to trace the transport of pollutants. Modelling results show no significant pollution even for worst case scenarios from the radioactive waste dumped in the Kara Sea to other seas in the Arctic or North Atlantic (as in Harms 1997). The results from the dispersion models suggest that, even for worst case scenarios, the contamination of Arctic waters and North Atlantic areas is relatively minor compared to pre-contamination from Sellafield, or global fallout from nuclear weapon testing in the 1960s. Long range simulations of Sellafield discharges of ^{137}Cs since the 1960s correlates well with measured levels. Harms et al. (2000) investigated the role of Siberian river runoff for the transport of possible river contaminants in the Arctic Ocean. 3-D coupled ice-ocean models of different horizontal resolution were applied to simulate the dispersion of river water from the Ob, Yenisei and Lena. Circulation model results explain the main pathways and transit times of Siberian river water in the Arctic Ocean. Kara Sea river water clearly dominates in the Siberian branch of the Transpolar Drift, while the water from the Lena dominates in the Canadian Branch. The model confirms that contaminant transport through sediment laden sea ice offers a short and effective pathway for pollutant transport from Siberian rivers to the Barents and Nordic seas. Karcher et al. (2004) have compared the simulated dispersion of ^{99}Tc in surface water from the sources to the Nordic Seas and the Arctic Ocean as calculated by a hydrodynamic model and in assessment box model with field-observations from 1996 to 1999 to study concentrations, pathways and travel times. The observations cover the northern part of the Nordic Seas. The main sources of ^{99}Tc are global fallout from nuclear weapon testing, and discharges from reprocessing plants for spent nuclear fuel in Northwestern Europe. Radioactive wastes have been discharged from the reprocessing plant at Sellafield (UK) into the Irish Sea, and at La Hague (France) into the English Channel since 1952 and 1966 respectively. The model results were consistent with the observations and have shown typical pathways of dissolved radionuclides from the Irish Sea via the North Sea along the Norwegian coast. The results of the hydrodynamic model have indicated a large variability of surface concentrations in the West Spitsbergen Current.

The importance of sea ice for the climate has led to many efforts to develop different models which study sea-ice morphology, dynamics and thermodynamics of sea ice. Many papers, e.g. Zwally and Walsh (1987), Barry et al. (1993), Zhang et al. (2003), give very good overviews of sea ice modelling. Some comparisons between different modelling approaches and results are given in Pavlov et al. (2004). Large-scale sea ice modelling requires effective use of commensurate observational data sets (sea ice concentration, sea ice extent, sea ice motion) on daily to inter-annual timescales for initialisation and verification. Recent sea ice observation data, measured by satellites, combined with sea ice motion derived from buoys in the International Arctic Buoy Programme (IABP), initiated a large number of studies of ice motion and variability of ice conditions in the Arctic Ocean. This also includes the problem of pollutant transport by sea ice, and provides a good opportunity to develop, compare and verify sea ice models (Pfirman et al. 1997).

Here we discuss the results of our simulation of the transport of passive non-conservative tracers by currents from a number of possible sources in the Arctic Ocean and Nordic seas. For simulation vectors of ocean currents we used a 3-D baroclinic ocean model developed at the Arctic and Antarctic Research Institute (AARI, St.Petersburg, Russia). Model is documented in Pavlov (1995) and Pavlov and Pavlov (1999).

We also include the possible transport of contaminants via sea ice. To estimate the transport of passive tracers by sea ice from potential sources of contamination in the Arctic Ocean we used the Ice Statistical Model (ISMO) developed at the Norwegian Polar Institute (Korsnes et al. 2002; Pavlov et al. 2004). The main approach of ISMO is to reveal the statistical relationship between atmospheric forcing and sea ice conditions derived from satellite imagery, in order to reconstruct the ice drift and ice concentrations, estimate the sea ice fluxes through the main straits in the Arctic Ocean and Arctic marginal seas and calculate forward and backward trajectories of the ice drift from any point in the Arctic Ocean.

18.2 Methods and data

18.2.1 Model of the dispersion of contaminants by ocean currents

To model the dispersion of a soluble contaminant we use the 3-D Eulerian transport equations for a non-conservative passive tracer with properties corresponding to anthropogenic radionuclides such as ^{137}Cs and ^{90}Sr.

$$\frac{\partial c}{\partial t} + u\frac{\partial c}{\partial x} + v\frac{\partial c}{\partial y} + w\frac{\partial c}{\partial z} = -\lambda c + \frac{\partial}{\partial z}\eta\frac{\partial c}{\partial z} + \mu\Delta c + Q\delta(r - r_0) \tag{1}$$

where c is the contaminant concentration; u,v,w are the components of the current velocity in the x, y and z directions; λ is the decay constant; η is the vertical diffusion coefficient; μ is the horizontal diffusion coefficient; $r_0=(x_0,y_0,z_0)$ gives the co-ordinates of the source; δ is Dirac delta function; and Q is the source strength.

Initial conditions are c=0 at t=0 and the boundary conditions are:

$$\frac{\partial c}{\partial n} = 0 \qquad u_n \geq 0; \qquad\qquad c = 0 \qquad u_n < 0 \tag{2}$$

where u_n is the projection of the current speed vector to the external normal to the surface S, restricting the calculation area. These conditions allow for the transport of a contaminant out of the model domain. In general Eq. (1) describes two different physical processes. The first is the transfer of a substance, with its conservation along the trajectory (LHS Eq. (1)) and is described by the equation:

$$\frac{\partial c}{\partial t} + u\frac{\partial c}{\partial x} + v\frac{\partial c}{\partial y} + w\frac{\partial c}{\partial z} = 0 \tag{3}$$

The second physical process is connected with the diffusion of the substance and its disintegration in the process of spreading from the source (RHS Eq. (1)) and is described by the equation:

$$\frac{\partial c}{\partial t} = -\lambda c + \frac{\partial}{\partial z}\eta\frac{\partial c}{\partial z} + \mu\Delta c + Q\delta(r - r_0) \tag{4}$$

Marchuk (1982) has shown that splitting the initial Eq. (1) into the two Eqs. (3) and (4), by physical processes, gives a form more suitable for numerical application. Eq. (4) is discretized as finite differences on an Arakawa C-grid and Eq. (3) is solved by the “Flux-Corrected Transport” (FCT) method (Boris and Book 1973) which has low viscosity whilst preserving the monotone and conservative character of the tracer field.

Horizontal and vertical velocities of currents for Eq. (1) were simulated using a 3-D baroclinic ocean level-type model (Pavlov and Pavlov 1999). The model is based on the Boussinesq approximation of the non-linear primitive equations of motion. Model equations including the sea ice parameterisation and numerical methods are in detail described in Pavlov and Pavlov (1999). The Arctic Ocean model has 22 layers in the vertical scale. We used a spherical rotated grid with a spatial resolution of 55 km. The model was driven with monthly mean climatologic atmospheric pressure and wind calculated from NCEP/NCAR gridded data (http://dss.ucar.edu/datasets/) and 3-D seasonal mean potential density calculated from data in the US-Russian atlas (US-Russian Joint Atlas 1996). The climatologic annual cycle of the discharge of the major rivers into the seas of the Arctic Ocean (Ivanov 1976; Omstedt et al. 1994) and data on water exchange through the Bering Strait and straits of the Canadian Archipelago were used to assign boundary conditions at open boundaries. Mean water exchange values through Bering Strait are sufficiently well known and estimates by different authors for different times are very close. For this model the water transport through Bering Strait was prescribed to be 1.2 Sv in summer and 0.7 Sv in winter (Pavlov and Pavlova 1999). The water transport from the Arctic Ocean through the Canadian Archipelago straits is taken from Coachman and Aagaard (1988) to be 2.0 Sv. The water exchange at open boundaries in the straits between Greenland and Iceland and between Iceland and the European continent were not prescribed, but the emission condition for the vertical-averaged horizontal velocity $\bar{u}$ was assumed to be $\bar{u} = \xi (g/h)^{1/2}$, where ξ -sea level elevation, g - Earth gravity acceleration and h-depth.

The annual cycle of all forcing and boundary conditions was not changed during the simulations and as a result after about 30 years we obtained a stable annual cycle of the 3-D water circulation in the Arctic Ocean. Harms et al. (2000) using a similar approach achieved a stable seasonal cycle in the ice and the upper ocean circulation after 35-years running their coupled ice-ocean model of the Arctic Ocean. The annual cycle of the water circulation obtained is used in the integration of Eq. (1).

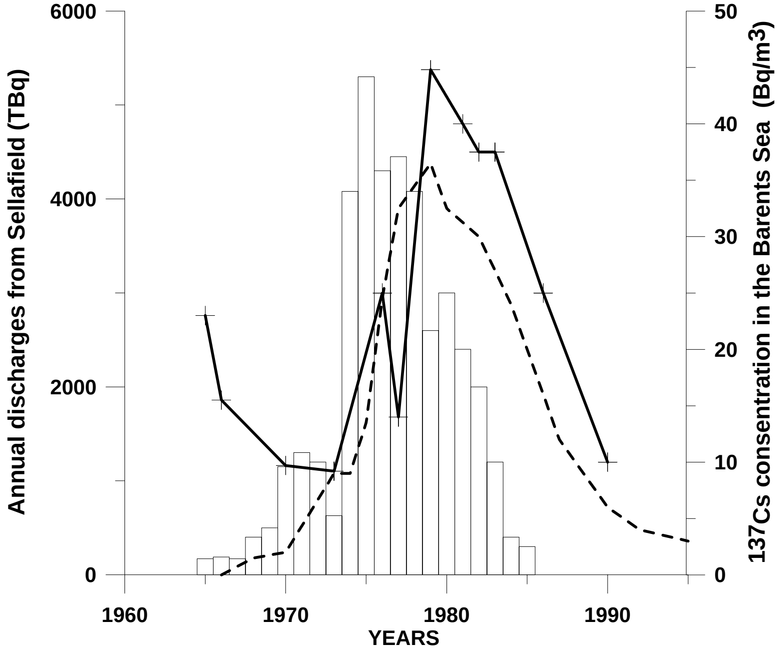

Fig. 18.1. Annual discharge (TBq) of ^{137}Cs from Sellafield (bars); ^{137}Cs concentration (Bq m^{-3}) in the Barents Sea surface waters. Observations from Kershaw and Baxter (1995)-solid line, and modelling results-dashed line (Kulakov and Pavlov 1999)

Kulakov and Pavlov (1999) have verified this model using data on the release of ^{137}Cs from the Sellafield reprocessing plant into the Irish Sea on the Cumbrian coast of England. The discharge from Sellafield started in 1952 (Dahlgaard 1995; Israel et a1. 1993; Matishov et al. 1994; Smith et al. 1990, 1998; Smith and Ellis 1999) and peaked in the mid- to late-1970s (Fig. 18.1). Almost all ^{137}Cs entering the sea with waste from Sellafield was transported from the Irish Sea to the North and Norwegian seas and then via the North-Atlantic Current to the Barents Sea and the Arctic Ocean. This passage has been well described previously; summary is presented in Kershaw and Baxter (1995). Using this model the redistribution and transformation of ^{137}Cs from the source in coastal water of the British Islands was calculated for 30 years from 1965 to 1995 with a time interval of one day. The strength of the source was prescribed in accordance with the real discharge volumes (Fig. 18.1). For the calculations the coefficients of the vertical and horizontal diffusion were assumed to be equal to 5 and $2 \cdot 10^5$ cm^2/s respectively. Kulakov and Pavlov (1999) reported that the calculated ^{137}Cs distribution is both qualitatively and quantitatively close to that in the Nordic seas (Kershaw and Baxter 1995; Vakulovsky et al. 1993).

Fig. 18.1 shows the comparison of the observed and the calculated time variations of the levels of ^{137}Cs concentrations in the surface water of the Barents Sea. Good agreement suggests that the model describes well the processes of transfer and transformation of ^{137}Cs.

18.2.2 Model of the sea ice transport

Sea ice trajectories have been simulated by the ISMO which was well documented in Korsnes et al. (2002) and Pavlov et al. (2004). In the development of ISMO, a multiple linear regression model was used to establish the statistical relationship between: 1) ice motion and the spatial structure of the sea level atmospheric pressure (SLP); and 2) sea ice concentration and both sea surface temperature (SST) and the spatial structure of the sea level pressure (SLP) in the each point of simulating domain.

The following observational data was used for statistical analysis: Monthly mean sea ice concentration and ice drift from the Special Sensor Microwave /Imager data set from the EOS Distributed Active Archive Center (DAAC) at the National Snow and Ice Data Center, University of Colorado, Boulder, CO. Monthly mean gridded sea level atmospheric pressure (SLP) fields and sea surface temperature (SST) from the NCEP/NCAR data set.

This model was verified by comparing simulated and observed ice conditions such as ice drift, ice concentration, ice fluxes through the main straits of the Arctic Ocean and ice tracks. The comparisons showed quite good agreement between the ISMO results and the observational data, and also with results of other models (see Pavlov et al. 2004). Using the ISMO we have computed the vectors of ice velocity for the period 1899-2000.

18.3 Contaminant Transport

18.3.1 Dispersion of passive tracers by water from potential sources of contaminants

Numerical experiments simulating the transport of contaminants from possible sources in different parts of the Arctic Ocean have been performed using calculated 3-D current fields. For these simulations potential pollut-

ant sources have been located in the vicinity of river-mouths of major rivers flowing into the Arctic Ocean, as well as in the Bering Strait, in the bottle-neck of the White Sea, in the Faeroe-Shetland Channel and also in the region of the wreck of the “Komsomolets” nuclear submarine.
What is the reason of such chooses?

The Faeroe-Shetland Channel (not far from the Sellafield reprocessing plant), the nuclear submarine wreck “Komsomolets” as well as the Kara Sea with the Ob and Yenisei river mouths, are chosen due to the public, political and scientific concern, and because there are many papers and reports already published from these sites.

The cumulative, and decay corrected total ^{137}Cs radioactivity released in Sellafield amounts to approximately 40 PBq, 14 PBq of which entered the Arctic regions mainly through the Faeroe-Shetland Channel. Maximum releases from Sellafield occurred in 1975. Releases of ^{137}Cs have been continually reduced since that time (Kershaw and Baxter 1995).

Radioactive sources dumped in the Kara Sea mainly include 17 nuclear ship reactors, seven of them still containing spent fuel. The total radioactive inventory at the time of dumping was 37 PBq (Yablokov Commission Report 1993; NPRA 1996; AMAP 1998). By 1994 this had decayed to approximately 4.7 PBq. The dominant nuclides are ^{137}Cs, ^{90}Sr, ^{63}Ni and ^{241}Pu. The amount of ^{137}Cs is estimated to be approximately 1 PBq for 1994 (IAEA 1997).

The sunken submarine “Komsomolets” contains one nuclear reactor with an inventory of long lived radionuclides comprising of 2800 PBq of ^{90}Sr and 3100 PBq of ^{137}Cs. Two nuclear torpedoes with mixed uranium/plutonium warheads, situated in the forepart of the hull contain about 16 PBq of weapons-grade plutonium (AMAP 1998).

The Kara Sea is distinguished from the other Siberian shelf seas by the strong influence of continental discharge. It receives about 55 % (1290 km^3/year) of the total river runoff discharged to the entire Siberian Arctic. The annual discharge from the Ob River is 400 km^3 and from the Yenisei River is 630 km^3 (Soviet Arctic 1970; Pavlov and Pfirman 1995). The nuclear fuel reprocessing plant Mayak is situated around the headwaters of the river Techa, which ultimately drains into the Kara Sea via the Ob River. The waste management system has been developed on a series of natural and artificial reservoirs and drainage canals. A total of 4000 PBq (decay corrected to 1994) comprising mainly of ^{90}Sr and ^{137}Cs has been released to this restricted system (NRPA 1997). Tomsk reprocessing plant also enters the drainage basin of the Ob. The plant’s storage ponds contain an estimated 4800 PBq. The storage ponds at Krasnoyarsk reprocessing plant are believed to contain an inventory of about 2 PBq. As at the other sites, there is a risk of contaminated groundwater migrating into the rivers, in this case the Yenisei river. (AMAP 1998). The observations carried out by Roshydromet, Russia (Vakulovsky et al. 1993) indicate that the amount of ^{90}Sr transported by the Ob during 1961-1989 is about 1 PBq, and 0.1 PBq ^{137}Cs.

In contrast to the possible sources of contamination mentioned above, information about contaminant levels at other possible sources such as the Lena, Kolyma and Mackenzie river mouths, the bottle-neck of the White Sea and the Bering Strait are fragmental or practically absent.

The large rivers of Siberia such as Lena and Kolyma, and Mackenzie in Canada transport large amounts of water over long distances and on their way to the Arctic seas. The annual discharge of the Lena and Kolyma is 525 km^3 and 132 km^3, respectively, and the Mackenzie runoff is 333 km^3/year (AMAP 1998). These areas include agricultural and industrial regions, and also regions of mining, and oil and gas explorations in Siberia and Canada. So, these rivers are expected to be a key source for considerable quantities of several different contaminants

About 1 Sv enter the Arctic Ocean from the Pacific Ocean with the Pacific current through the Bering Strait (Pavlov and Pavlova 1999). These waters wash the industrial regions of the Russian Far East and Northern America where possible sources of contamination are located, such, for example, as the large shipyards for nuclear-powered submarines near Vladivostok, and the regions of drilling activity in Alaska.

The bottle-neck of the White Sea was chosen because the city of Severodvinsk lies on the delta of the Dvina River, close to Archangelsk, and has one of the largest shipyards for nuclear-powered submarines in the former Soviet Union. It is also a disposal site for military nuclear waste (Nilsen and Bøhmer 1994; Champ et al. 1998). Severodvinsk is potentially a major source of radioactive contamination in the White Sea.

However, even if we do not have information about contaminants from these regions, the selected sources could release large amounts of contaminants in the future. For example, release of contaminants through accidents during production, transport, waste disposal and storage, oil and gas exploration and exploitation, and also nuclear submarine waste generated from operations in the Northwest and Far East, or accidents involving nuclear weapons. Potential contaminant release that may occur in the Arctic in the future and source related assessments of potential release are well documented in AMAP (1998).

As we do not have information about a possible release volume, pollutant concentration in all these sources has been set to 100 arbitrary units. The non-conservative parameter has been prescribed to 30 years, this being approximately equal to the averaged half-life of the dangerous anthropogenic long-life radionuclides, such as ^{137}Cs and ^{90}Sr.

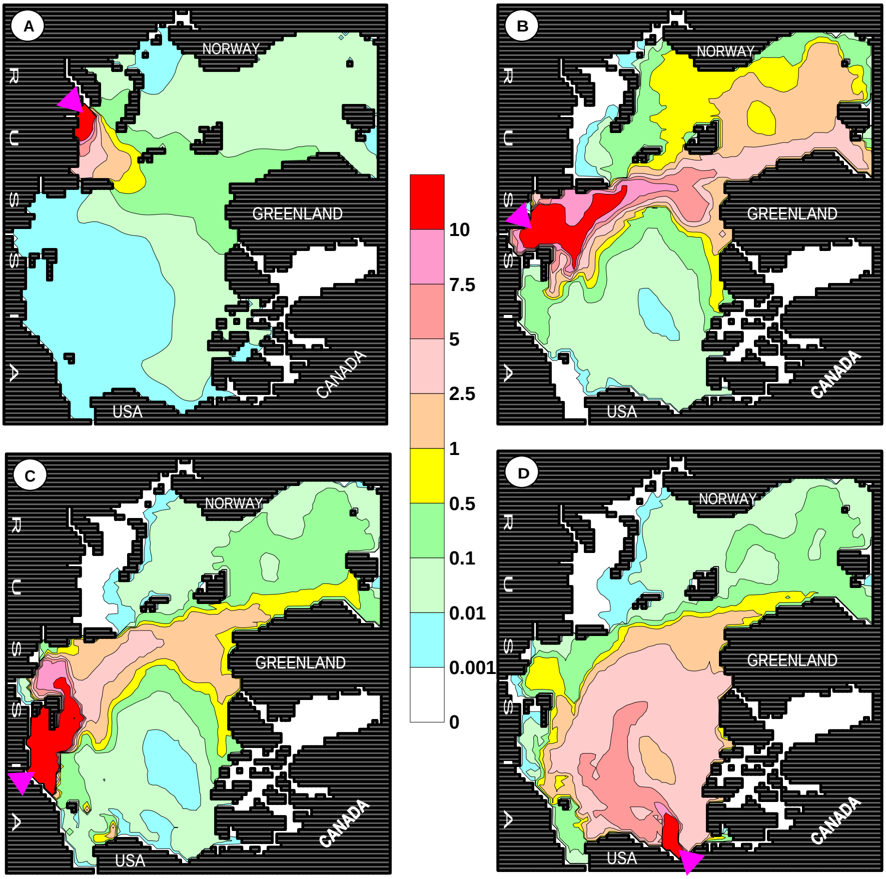

Fig. 18.2. Distributions of pollutant concentration in the surface layer of the Arctic Ocean after 15 years of release from sources in the river-mouths of the major rivers: A - Ob and Yenisei rivers, B - Lena river, C - Kolyma river, and D - Mackenzie river. The scale shows % of pollutant in relation to its concentration at source. ▲ - source location.

Distributions of the pollutant concentration from all the permanently acting sources in the river-mouths of major rivers in the surface layer of the Arctic Ocean after 15 years from the beginning of the release are presented in Fig. 18.2. Depths of the sources near the river-mouths have been set equal to 5 m.

Pollutant spreading from sources in the river mouths of the Siberian shelf is directed predominantly to the north-west. Pollutants from the source in the Kara Sea in the region of the Ob-Yenisei river mouth (Fig. 18.2a) cover a greater part of the Nordic seas, the Laptev Sea and the area near the northern coast of Greenland. However, pollutant concentrations exceeding 5% of the source concentration in the surface layers of the ocean are only observed within the Kara Sea area. The most rapid spreading of the pollutant is observed from the source near the Lena river mouth (Fig. 18.2b). The pollutants entering the Transpolar Drift are transported to the coast of Greenland, spreading later over the region of the Nordic seas. Pollutant concentrations of 5% are observed in the Fram Strait and near the northern coast of Greenland.

The structure of the pollutant transportation from the source near the Kolyma river mouth (Fig. 18.2c) is in many ways similar to the previous one. However, in this case contamination of the Nordic seas significantly decreases, and contamination of the coastal zone of the East Siberian and Chukchi seas increases. As this takes place concentrations exceeding 5% are registered along the continental slope and in the south-eastern part of the Laptev Sea and in the coastal zone of the East Siberian Sea. Pollutants from the source near the Kolyma river mouth are transported also along the continental slope to the east in the sub-bottom layer. They reach the sea surface in the Chukchi Sea to the north of Wrangel Island and near the north-east coast of Alaska. A pollutant concentration of 5% of the source is registered in this region, whereas on the surface of the northern part of the East Siberian Sea, along the transportation route of the pollutants, their concentration is less than 3%. A completely different situation occurs in the case where the pollutant spreads from a source located in the Mackenzie river mouth (Fig. 18.2d). The pollutants in this case essentially fill the region of the anticyclonic gyre, and only an insignificant part of them enters the Laptev Sea and Nordic seas. Pollutant concentrations exceeding 5% are observed in the surface layers in the anticyclonic gyre in the Canadian Basin.

In the second set of numerical experiments, pollutant with 100% concentration are released in the region of the wreck of the “Komsomolets” nuclear submarine in the sub-bottom layer at the depth 1700 m, in the bottle-neck of the White Sea, in the Faeroe-Shetland Channel and in the Bering Strait in the streams of the Atlantic and Pacific currents, respectively, at the depth 5 m. The pollutant-spreading from these sources after 15 years from the beginning of their activity is given in Fig. 18.3.

The pollutants from the “Komsomolets” wreck region crop out at the surface mainly in the area of the central part of the Barents Sea and the north-western part of the Kara Sea (Fig. 18.3a). Regions with concentrations higher than 5% are located near the north-western part of Norway. The pollutants from the source in the surface layer near the bottleneck of the White Sea (Fig. 18.3b) spread to the east along the coasts of the Barents and Kara seas and to the north along the western coast of Severnaya Zemlya.

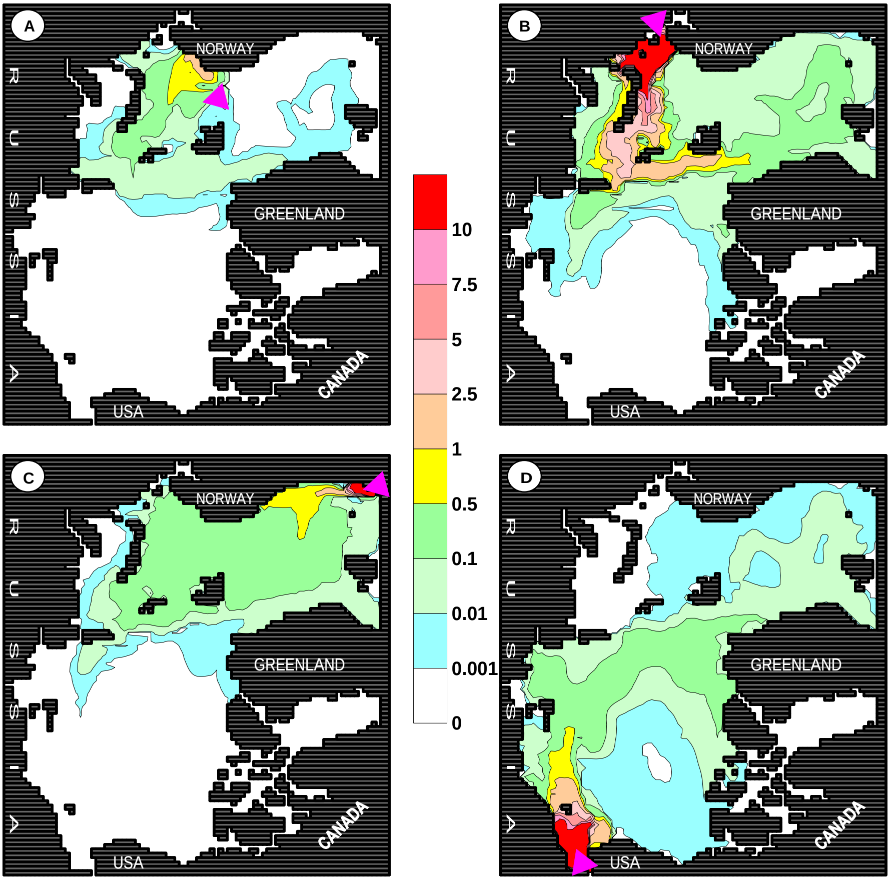

Fig. 18.3. The spread of a pollutant with ocean currents, 15 years after the beginning of a hypothetic pollutant release, from sources located in the following regions: A - the wreck of the "Komsomolets" nuclear submarine, B - the bottle-neck of the White Sea, C - the Faeroe-Shetland Channel in the stream of the Atlantic current and D - the Bering Strait. The scale shows % of pollutant in relation to its concentration at source. ▲ - source location.

Having entered the Transpolar Drift Stream in the northern part of the Kara Sea the pollutants subsequently reach the Greenland Sea. Pollutant concentrations exceeding 5% are registered in the eastern and south-eastern parts of the Barents Sea, in the Kara Sea and in the stream of the Transpolar Drift.

The pollutants from the possible source in the stream of the North Atlantic Current in the Faeroe-Shetland Channel (Fig. 18.3c) spread predominantly in the Norwegian and Barents seas and in the northern part of the Kara Sea. A region with concentrations higher than 5% in the surface layer is observed in the Norwegian Sea, in the western part of the Barents Sea and near the southern and western coasts of Spitsbergen.

The pollutants from the possible source in the Bering Strait (Fig. 18.3d) spread mainly to the west. The zone of possible contamination covers the Chukchi Sea, the northern part of the East Siberian Sea, the greater part of the Laptev Sea and the region of the Transpolar Drift Stream. Pollutant concentrations exceeding 5% are registered in the Chukchi Sea and in the north-eastern part of the East Siberian Sea. Concentrations of 10% and above are located in the Bering Strait and in the Chukchi Sea near the coasts of Alaska and Chukotka.

The numerical experiments performed revealed that the anticyclonic gyre zone in the Canadian Basin would be the least polluted area of the Arctic Ocean for the contamination sources located in the coastal zone of the Siberian shelf seas, the Barents and Norwegian seas.

There are some regions that would become contaminated in nearly all possible variants of location of the possible sources in the coastal zone of the Arctic seas. Among these are the Laptev Sea and the northern and eastern coasts of Greenland. This could explain measured increased concentration of the anthropogenic radionuclides in the Greenland coastal waters, for example a sharp increase in the concentration of ^{137}Cs near Danmarkshavn from 1986 (3.5 Bq m^{-3}) to 1989 (>8 Bq m^{-3}) (Dahlgaard 1995; Pavlov and Stanovoy 2001).

18.3.2 Sea ice transport from potential sources of contaminants

Here we continue the analysis of the simulation results described by Pavlov et al. (2004). In Pavlov et al. (2004), in order to estimate the drift route of the sea ice from the areas containing potential sources of pollution in the Arctic Ocean, trajectories of the ice drift were simulated. The following regions were chosen: in the Kara Sea–the regions of the Ob and Yenisei river mouths; in the Laptev Sea–the region of the Lena river mouth; in the East Siberian Sea–the region of the Kolyma river mouth; in the Chukchi Sea–the region near the Bering Strait; and in the Beaufort Sea–the mouth of the Mackenzie River. For these simulations reconstructed ice drift data for the period 1899-2000 were used. Trajectories were started for each month that the ice concentration at the starting position was more than 10%. Most of the trajectories were launched in the arctic winter time. In this work, based on trajectories simulated in Pavlov et al. (2004) from different potential sources in the Arctic Ocean, we analyse and discuss interannual variability of the travel time (TT) from all selected sources, and

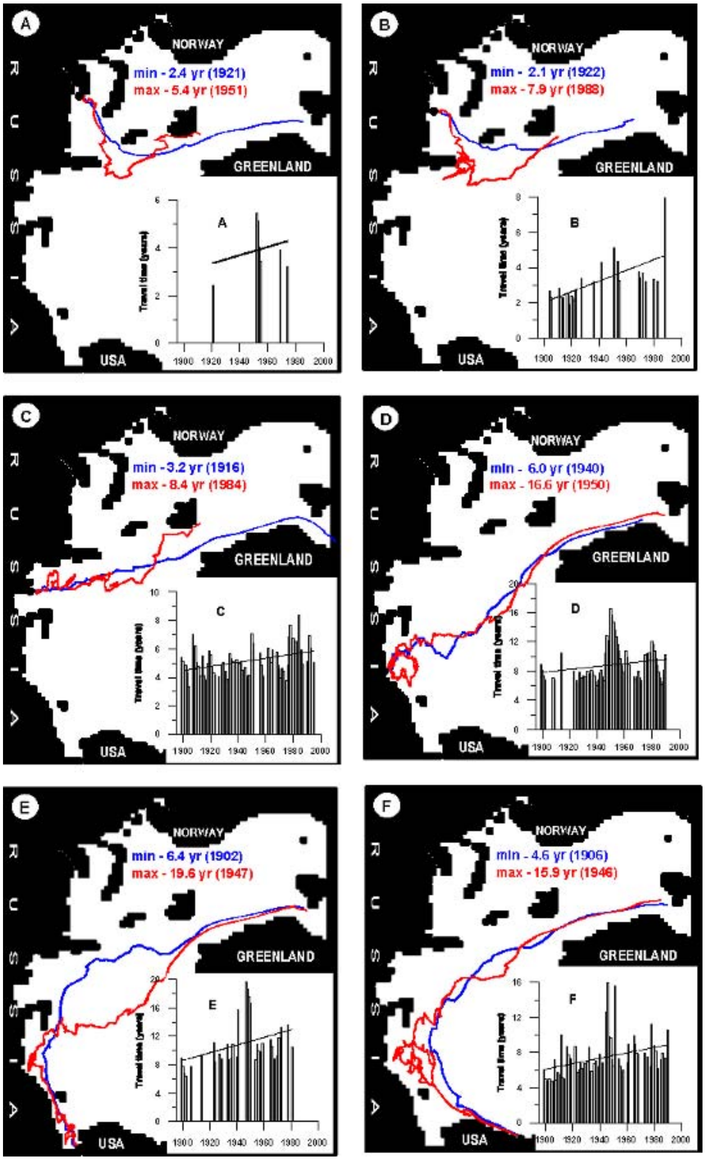

Fig. 18.4. Trajectories for sea ice drift with the minimum (blue) and maximum (red) travel time from selected potential sources to the Fram Strait region (80ºN). A-Ob River, B-Yenisei River, C-Lena River, D-Kolyma River, E-the Bering Strait and F-Mackenzie river. Bar diagrams show the travel time to the Fram Strait for sea ice starting in different years in the last century (1899-2000).

estimate the shortest and longest trajectories of ice drift.

Fig. 18.4 shows maps with trajectories and the travel time from selected potential sources to the Fram Strait (FS) for sea ice starting in different years in the last century (1899-2000). Trajectories with the minimum and maximum TT are also shown. For example, sea ice from the sites in the Kara Sea reaches the FS after 2-4 years (Fig. 18.4a, b). The probability of ice from the Ob Gulf region reaching the FS is only 0.7%. From the Yenisei Gulf region the probability is increased to 27%. The most probable route from these sites to the Barents Sea is through the strait between the islands of Novaya Zemlya and Franz Josef Land (Pavlov et al. 2004). Ice starting from the Ob Gulf in 1921 has the shortest TT to the FS. It drifts from the Ob Gulf to the north and around the northern coasts of Franz Josef Land and Svalbard to reach the FS in 2.4 years (Fig. 18.4a).

Ice starting in 1954 has the longest TT (5.4 years). The ice from this area drifts to the north-east, then west near the northern coast of Severnaya Zemlya, and then along the northern coast of Svalbard through the eastern part of the FS. A similar configuration of trajectories with the minimum and maximum TT was simulated for ice drifting from the Yenisei Gulf in 1922 (TT 2.1 years) and in 1988 (7.9 years). The trajectory starting in 1988 reached the north-western part of the Laptev Sea and the ice drifted for a long time near the northern coast of Severnaya Zemlya (Fig. 18.4b). The sea ice from the Laptev Sea (Fig. 18.4c) takes roughly 4-8 years to reach the FS and the probability of this happening is 71%. The trajectory with the shortest TT (3.2 years) started in 1916, when the ice drifted directly to the western part of the FS (Fig. 18.4c). The trajectory with the longest TT (8.4 years) started in 1984. This trajectory has the same general direction but a very complicated configuration, ending up in the eastern part of the FS (Fig. 18.4c). The longest TT is from the Kolyma river mouth (Fig. 18.4d) and the Bering Strait region (Fig. 18.4e).

The TT of the sea ice drift from the Kolyma River ranges form 7-17 years with a probability of reaching the FS of 71%. The ice drift trajectories with the shortest (6.0 years) and the longest (16.6 years) TT are both from the area of the Kolyma river delta. They both pass the North Pole and continue to the south and the western part of the FS. However the trajectory with the longest TT, starting in 1950, has a much more complicated configuration (loops at the shelf of the East Siberian Sea) than the trajectory with the shortest TT, starting in 1940. For ice starting from the Bering Strait, TT ranges between 5-19 years (Fig. 18.4e) and the probability of reaching the FS is decreased to 41%. The trajectory with the shortest TT (6.4 years) started in 1902. It runs along the coast of Siberia, through the De Long Strait and to the northern part of the Laptev Sea along the continental slope. From Severnaya Zemlya island the ice drifts west and southwest to the FS. The trajectory with the longest TT (19.6) started in 1947 and it has a more eastern position in the centre of the Polar Basin (Fig. 18.4e). Ice drifts a long time at the shelf zone of the Chukchi and East Siberian seas. From the site near the Mackenzie River (Fig. 18.4d) sea ice can reach the FS in 5-16 years with a probability of 68% of this happening. Trajectories with the shortest (4.6 yr) and longest (15.9 yr) TT have nearly the same position, but the configuration of the trajectory with the longest TT is much more complicated. Based on analysis of the patterns of the atmospheric circulation (not shown) we can conclude that the shortest TT of ice drift to the FS is connected with the extreme development of anticyclonic circulation above the Arctic Ocean. During the longest TT the atmospheric circulation is in an extreme cyclonic regime.

In the light of climate change in the Arctic it is interesting to consider the inter-annual variability of the TT of ice drift through the Arctic Ocean. We have obtained a generally positive trend (Fig. 18.4). The minimum TT was in the first two decades of the last century. In the last four decades the TT has increased. Maximum values of the TT were obtained at the end of the 1940s and mid 1950s, except for ice drifting from the Lena River where the maximum was at the end of the 1970s and beginning of the 1980s.

These calculated trajectories and TT estimations are in good agreement with the results of Pfirman et al. (1997; 2004a).

The studies of Pfirman et al. (1997) have indicated that drifting Arctic sea ice plays an important role in the redistribution of sediments and contaminants. It was also shown that forward and backward trajectories of sea ice can be calculated to identify regions influenced by sea ice from different source areas and reconstruct the drift path of individual ice floes with some confidence over a period of several years. Authors have demonstrated that ice from the Kara Sea has a strong influence on the Laptev Sea, Barents Sea, Svalbard, the southern portion of the Transpolar Drift Stream, and eastern FS. Ice from the Laptev Sea is mostly advected through the FS and to a lesser degree into the Barents Sea. Ice from the East Siberian Sea is either advected through the FS or is caught up in the Beaufort Gyre and is transported along the northern North American coast. Pfirman et al. (2004a) have analysed sea ice drift from 1979 to 1997 based again on fields of ice motion obtained from IABP. The analysis of potential trajectories of sea ice incorporated in the central Arctic pack between 1979 and 1997 showed extensive changes in the fate of sea ice exported from the Arctic shelves. TT of ice within the central Arctic Basin decreased by at least 1 year, at the same time that the fraction of ice with 4 year TT exported through the FS increased. Ice from distant sources that formerly recirculated in the Beaufort Gyre under lower NAO/AO conditions of the 1980s, was exported more directly through the FS in higher NAO/AO conditions of the 1990s. It was recognised that changes in trajectories of ice with different origins are important, because they affect advection and release of any transported material.

However, in contrast to the ISMO approach for simulation of sea ice trajectories, Pfirman et al. (1997; 2004a) have calculated trajectories based on historical drift data from IABP. Buoy positions have high spatial accuracy and temporal resolution. But the spatial distribution is generally rather coarse, so that buoy data provide only a highly restricted view of the temporal and spatial variability of the large-scale sea ice drift patterns. Buoy data provided by the IABP cover mostly the central part of Arctic Ocean, so in significant areas of the Siberian seas, where there are potential sources of pollution, the buoy data are absent.

18.4 Conclusions

The most rapid spreading of the pollutants and largest contaminated areas result from possible sources located near the Lena and Mackenzie river mouths.

There are two regions, the northern and eastern coastal zone of Greenland and the Laptev Sea, that are contaminated in nearly all variants of location of the possible sources in the coastal zone of the Arctic and Nordic seas.

The calculated trajectories of ice drift from areas of potential sources of pollution allow us to evaluate the character of pollutant transport and the areas of redistribution. From that we can conclude that sea ice from most potential sources of contaminant can reach the open Polar Basin and the FS. Contaminated sea ice from potential sources in the Kara and Laptev seas can reach FS within 2-4 years and from the East Siberian, Chukchi and Beaufort seas within 6-11 years.

Analysis of the inter-annual variability of sea ice TT from different sites to FS has shown a significant positive trend in the last century.

The results of the simulation can also give useful information for the selection of the most representative areas for monitoring contaminants in the Arctic Ocean. Based the structure of passive tracer spreading we obtained and our simulated trajectories of ice drift from different potential sources in the Arctic Ocean we conclude that the most important regions for monitoring of contaminants are FS and Laptev Sea.

Acknowledgements

Support for this work was provided by the Transport and Effects Programme, Phase 2 (financed by the Norwegian Ministries of Environment and of Foreign Affairs). Partly the work was supported by the Barents Sea Production Licenses 182, 225 and 228 (Norsk Hydro, Statoil, Agip, Chevron, Fortum, Petero and Enterprise - contract no. 9000000465).

References

Aarkrog A (1993) Radioactivity in polar regions-main sources. In: Strand P, Holm E (Eds) Environmental Radioactivity in the Arctic and Antarctic, Norwegian Radiation Protection Authority, Østerås, Norway, pp 15-34

AMAP (1998) AMAP Assessment Report: Arctic Pollution Issues. Arctic Monitoring Assessment Programme (AMAP), Oslo, Norway

AMAP (1997) Arctic Pollution Issues: A State of the Arctic Environment report., Arctic Monitoring Assessment Programme (AMAP), Oslo, Norway

ANWAP (1997) Radionuclides in the Arctic Seas from the Former Soviet Union: Potential Health and Ecological Risks. Office of Naval Research, Arlington, VA, USA

Barry RG, Serreze MC, Maslanik JA, Preller RH (1993) The Arctic sea ice-climate system: observations and modelling. Reviews of Geophysics 31(4):397-422

Boris JP, Book DL (1973) Flux-Corrected Transport I: SHASTA-A Fluid Transport Algorithm That Works. J Comput Phys 11:38-69

Champ MA, Makeyev VV, Brooks JM, Delaca TE, van der Horst KM, Engle MV (1998) Assessment of the Impact of Nuclear Wastes in the Russian Arctic. Mar Pollut Bull 35(7-12):203-221

Coachman LK, Aagaard K (1988) Transports through Bering Strait: Annual and Interannual Variability. J Geophys Res 93(C12):15535-15541

Dahlgaard H (1995) Transfer of European coastal pollution to the Arctic-radioactive-tracers. Mar Pollut Bull 31(1-3):3-7

Duursma EK, Carroll J (1996) Environmental Compartments, equilibria and assessment of processes between air, water sediments and biota. Spring-Verlag, Berlin, Germany

Emery WJ, Fowler CW, Maslanik JA, Pfirman S (1997) New satellite derived sea ice motion tracks Arctic contamination. Mar Pollut Bull 35(7-12):345-352

Harms I (1997) Modelling the dispersion of ^{137}Cs and ^{239}Pu released from dumped waste in the Kara Sea. J Mar Syst 13:1-19

Harms I, Karcher MJ (1999) Modeling the seasonal variability of hydrography and circulation in the Kara Sea. J Geophys Res 104(C6):13431-13448

Harms I, Karcher MJ, Dethleff D (2000) Modelling Siberian river runoff – implications for contaminant transport in the Arctic Ocean. J Mar Syst 27:95-115

IAEA (1997) Predicted radionuclide release from marine reactors dumped in the Kara Sea-report of the source team working group of the IASAP, IAEA-TECDOC-938, Vienna, Austria

Israel Y, Tsiban A, Vakulovsky S (1993) Radioactivity and Environmental Problems for the Seas and Ocean. Proc Radioactivity and Environmental Security in the Oceans: New Research and Policy Priorities in the Arctic and North Atlantic. Woods Hole Oceanographic Institution, June 7-9, 1993, Woods Hole, Massachusetts, USA:65-79

Ivanov V (1976) Fresh water balance of the Arctic Ocean. Rosgidrometeoizdat, Leningrad, Trudy AANII 323:138-148 (In Russian)

Karcher MJ, Gerland S, Harms IH, Iosjpe M, Heldal HE, Kershaw PJ, Sickel M (2004) The dispersion of ^{99}Tc in the Nordic Seas and the Arctic Ocean: a comparison of model results and observations. J of Environmental Radioactivity 74:185-198

Kershaw P, Baxter A (1995) The transfer of reprocessing wastes from north-west Europe to the Arctic. Deep-Sea Res II 42(6):1413-1448

Korsnes R, Pavlova O, Godtliebsen F (2002) Assessment of potential transport of pollutants into the Barents Sea via sea ice–an observational approach. Mar Pollut Bull 44(9):861-869

Kulakov MYu, Pavlov VV (1999) Modelling of consequences of damp of radioactive waste from Sellafield plant. Rosgidrometeoizdat, St.Petersburg, Trudy AANII 442:159-164 (In Russian)

Marchuk GI (1982) Mathematical modelling in respect of the environmental problem. Nauka, Moscow, Russia (In Russian)

Matishov G, Matishov D, Shipa Ye, Rissanen K (1994) Radionuclides in the ecosystem of the region of the Barents and the Kara Seas. Apatity, Murmansk, Russia (In Russian)

Nies H, Harms I, Karcher MJ, Dethleff D, Bahe C (1999) Anthropogenic radioactivity in the Arctic Ocean - review of the results from the joint German project. The Science of the Total Environment 237/238:181-191

Nilsen T, Bøhmer N (1994) Sources to radioactive contamination in Murmansk and Archangelsk counties. Bellona rapport 1994: 1, Miljøstiftelsen Bellona, Oslo, Norway

Nilsson A (1997) Arctic pollution issues: A state of the Arctic environment report. Arctic Monitoring Assessment Programme (AMAP), Oslo, Norway

NRPA (1996) Dumping of radioactive waste and investigation of radioactive contamination in the Kara Sea. Results from 3 years of investigations (1992-1994) in the Kara Sea. Joint Norwegian-Russian Expert Group for Investigation of Radioactive Contamination in the Northern Areas, Norwegian Radiation Protection Authority, Østerås, Norway

NRPA (1997) Sources contributing to radioactive contamination of the Techa river and areas surrounding the “Mayak” production association, Ural, Russia. Joint Norwegian-Russian Expert Group for Investigation of Radioactive Contamination in the Northern Areas, Norwegian Radiation Protection Authority, Østerås, Norway

Nürnberg D, Wollenburg I, Dethleff D (1994) Sediments in Arctic sea ice-entrainment, transport and release. Mar Geol 119:185-214
Omstedt A, Carmack E, Macdonald RW (1994) Modeling the seasonal cycle of salinity in the Mackenzie shelf estuary. J Geophys Res 99(C5):10011-10021
Pavlov VK (1995) Modelling of the Thermohaline Water Circulation of the Arctic Ocean. Proc of NDRE Workshop, Modeling Requirements for Water Mass Dynamics, Ice and River Transports in the Kara Sea, Workshop Norwegian Defence Research Establishment, Tjome, 26-30 June 1995, Norway: 200–224
Pavlov V, Stanovoy V (2001) The problem of transfer of radionuclide pollution by sea ice. Mar Pollut Bull 4:319-323
Pavlov VK, Pavlov PV (1999) Features of seasonal and interannual variability of sea level and water circulation in the Laptev Sea. In: Land-Ocean systems in the Siberian Arctic. Dynamics and history. Eds Kassens et al., Springer-Verlag, Berlin Heidelberg, pp 3-16
Pavlov VK, Pavlova OA (1999) Features of seasonal and interannual variability of thermohaline structure, currents and water exchange in the Bering Strait. Rosgidrometeoizdat, St.Petersburg, Trudy AANII 442:16-52 (In Russian)
Pavlov V, Pfirman S (1995) Hydrographic structure and variability of the Kara Sea. Deep-Sea Res II 42(6):1369-1390
PavlovV, Pavlova O, Korsnes R (2004) Sea ice fluxes and drift trajectories from potential pollution sources, computed with a statistical sea ice model of the Arctic Ocean. J Mar Syst 48(1-4):133-157
Pavlov VK, Kulakov MYu, Stanovoy VV (1995) Modeling of the transport and transformation of pollutants in the Arctic Ocean. Proc of NDRE Workshop, Modeling Requirements for Water Mass Dynamics, Ice and River Transports in the Kara Sea, Workshop Norwegian Defence Research Establishment, Tjome, 26-30 June 1995, Norway:225-249
Pfirman S, Haxby WF, Colony R, Rigor I (2004a) Variability in Arctic sea ice drift. Geophys Res Letters 31, L16402, doi:10.1029/2004GL020063
Pfirman S, Haxby W, Eicken H, Jeffries M, Bauch D (2004b) Drifting Arctic sea ice archives changes in ocean surface conditions. Geophys Res Letters 31, L19401, doi:10.1029/2004GL020666
Pfirman S, Colony R, Nürnberg D, Eicken H, Rigor I (1997) Reconstructing the origin and trajectory of drifting Arctic sea ice. J Geophys Res 102(C6):12575-12586
Preller RH, Cheng A (1995) Modeling the Dispersion of Radioactive Contaminants in the Arctic Using a Coupled Ice-ocean Model. Proc Arctic Nuclear Waste Assessment Program Workshop, Woods Hole Oceanographic Institution, Woods Hole, Massachusetts, 1-4 May, 1995
Rigor I, Colony R (1997) Sea-ice production and transport of pollutants in the Laptev Sea, 1979-1993. Science Total Environ 202:89-110
Rigor IG, Wallace JM, Colony RL (2002) Response of sea ice to the Arctic oscillation. J Clim 15:2648-2663
Scott EM, Gurbutt P, Harms I, Heling R, Nielsen SP, Osvath I, Preller R, Sazykina T, Wada A, Sjoeblom KL (1997) Benchmarking of numerical mod-

els describing the dispersion of radionuclides in the Arctic Seas. The Science of the Total Environment 202:123-134

Smith JN, Ellis KM (1999) Calculation features in the central Arctic Ocean revealed by nuclear fuel reprocessing tracers from Scientific Ice Expeditions 1995 and 1996. J Geophys Res 104(C12):29663-29677

Smith JN, Ellis KM, Jones EP (1990) Cesium 137 Transport Into the Arctic Ocean Through Fram Strait. J Geophys Res 95(C2):1693-1701

Smith JN, Ellis KM, Kilius LR (1998) ^{129}I and ^{137}Cs tracer measurements in the Arctic Ocean. Deep-Sea Res I 45(6):959-984

Soviet Arctic (1970) Seas and Islands of the Arctic Ocean. Nauka, Moscow (In Russian)

Vakulovsky S, Nikitin A, Chumichev V (1993) Radioactive Contamination of the Barents and Kara Seas. Proc Radioactivity and Environmental Security in the Oceans: New Research and Policy Priorities in the Arctic and North Atlantic. Woods Hole Oceanographic Institution, June 7-9, 1993, Woods Hole, Massachusetts, USA:157-169

US-Russian Joint Atlas (1996) Joint US-Russian Atlas of the Arctic Ocean, winter. National Snow and Ice Data Center, Environmental Working Group, Boulder, Colorado (on CD-Rom)

Yablokov AV (2001) Radioactive waste disposal in seas adjacent to the territory of the Russian Federation. Mar Poll Bull 43(1-6):8-18. This article extracts material from Yablokov Commission Report (1993)

Yablokov Commission Report (1993) Yablokov AV, Karasev VK, Rumyantsev VM, Kokeyev MYe, Petrov OL, Lytsov VN, Yemelyankov AF, Rubtsov PM (1993) Facts and Problems related to Radioactive Waste Disposal in Seas Adjacent to the Territory of the Russian Federation. Office of the President of the Russian Federation, Moscow

Zhang JL, Rothrock D, Steel M (2000) Recent changes in Arctic sea ice: The interplay between ice dynamics and thermodynamics. J Clim 13:3099-3114

Zhang JL, Thomas DR, Rothrock D, Lindsay RW, Yu Y (2003) Assimilation of ice motion observations and comparisons with submarine ice thickness data. J Geophys Res 108(C6),3170,doi:10.1029/2001JC0011041

Zwally HJ, Walsh JE (1987) Comparison of observed and modelled ice motion in the Arctic Ocean. Annals of Glaciology 9:136-144